

1 Predicting trends in atmospheric CO₂ across the Mid-Pleistocene

2 Transition using existing climate archives

3 Jordan R.W. Martin¹, Joel Pedro^{2,3}, Tessa R. Vance³

4 ¹Institute for Marine and Antarctic Studies, University of Tasmania, Hobart, 7004, Australia

5 ²Australian Antarctic Division, Kingston, 7050, Australia

6 ³Australian Antarctic Program Partnership, Institute for Marine and Antarctic Studies, University of Tasmania, Hobart, 7004,
7 Australia

8

9 *Correspondence to:* Jordan R.W. Martin (jrmartin@utas.edu.au)

10 **Abstract.** During the Mid-Pleistocene Transition (MPT), ca. 1250–800 kya, the Earth’s glacial cycles changed from 41 kyr to
11 100 kyr periodicity. The emergence of this longer ice-age periodicity was accompanied by higher global ice volume in glacial
12 periods and lower global ice volume in interglacial periods. Since there is no known change in external orbital forcing across
13 the MPT, it is generally agreed that the cause of this transition is internal to the earth system. Resolving the climate–carbon
14 cycle–cryosphere dynamics processes responsible for the MPT remains a major challenge in ice core and climate science. To
15 address this challenge, the international ice core community has prioritized recovery of an ice core record spanning the MPT
16 interval. The results from such ‘oldest ice’ projects are still several years away.

17 ~~Our objective here is to make an advanced prediction of atmospheric CO₂ out to 1.5 my. Our prediction utilizes existing records~~
18 ~~of atmospheric carbon dioxide (CO₂) from Antarctic ice cores spanning the past 800 ky along with the existing benthic water~~
19 ~~stable isotope (δ¹⁸O) record from marine sediment cores. Here we present results from a simple generalized least squares model~~
20 ~~that predicts atmospheric CO₂ out to 1.5 Myr. Our prediction utilizes existing records of atmospheric carbon dioxide (CO₂)~~
21 ~~from Antarctic ice cores spanning the past 800 kyr along with the existing LR04 benthic δ¹⁸O_{calcite} stack (Lisiecki & Raymo,~~
22 ~~2005) from marine sediment cores. Our predictions assume that the relationship between CO₂ and benthic δ¹⁸O–δ¹⁸O_{calcite} over~~
23 ~~the past 800 thousand years can be extended over the last one and a half million years. The implied implicit null hypothesis is~~
24 ~~that there has been no fundamental change in the global climate–carbon cycle–cryosphere feedback systems across the MPT.~~
25 ~~feedbacks between atmospheric CO₂ and the climate parameters represented by benthic δ¹⁸O_{calcite}, global ice volume and ocean~~
26 ~~temperature.~~

27 ~~We find that our predicted CO₂ record is significantly lower during glacial intervals than the existing blue ice and boron~~
28 ~~isotope based estimates of CO₂ that pre-date the continuous 800 ky CO₂ record. Our predicted glacial CO₂ concentrations are~~
29 ~~–9 ppm below glacial CO₂ concentrations observed in blue ice data at ca. 1 mya and –19 ppm below glacial CO₂ concentrations~~

30 reconstructed from boron isotopic data over ca ~1.1–1.25 mya. These results support rejection of our null hypothesis and
31 provide quantitative evidence of a fundamental shift in the global climate–carbon cycle–cryosphere feedback systems across
32 the MPT. However, the definitive test of the various theories explaining the MPT will be comparison of our predicted records
33 with the forthcoming oldest ice core records.

34 We test the GLS-model predicted CO₂ concentrations against observed blue ice CO₂ concentrations, δ¹¹B-based CO₂
35 reconstructions from marine sediment cores and δ¹³C of leaf-wax based CO₂ reconstructions (Higgins *et al.*, Yan *et al.*, 2019
36 and Yamamoto *et al.*, 2022). We show that there is not clear evidence from the existing blue ice or proxy CO₂ data to reject
37 our predictions nor our associated null-hypothesis. A definitive test and/or rejection of the null hypothesis may be provided
38 following recovery and analysis of continuous oldest ice core records from Antarctica, which is still several years away. The
39 record presented here should provide a useful comparison for the oldest ice core records and opportunity to provide further
40 constraints on the processes involved in the MPT.

43 1 Introduction

44 Ice core records from Antarctica provide comprehensive and continuous records of many climate parameters over the last
45 800 thousand years, e.g., the Vostok (Petit *et al.*, 1999) and European Project for Ice Coring in Antarctica’s Dome-C (EDC)
46 ice cores (Jouzel *et al.*, 2007). One of the major challenges in climate science lies beyond the current threshold of the ice
47 core record: The Mid-Pleistocene Transition (MPT), which spanned from ca. 1250–800 thousand years ago (kya) (Chalk *et*
48 *al.*, 2017). ~~The MPT and~~ is characterised by a change from regularly paced 40 thousand year (kyr) 40 ky glacial cycles with
49 thinner glacial ice sheets to quasi-periodic 100 ky glacial cycles in which ice sheets are more persistent and thicker (Clark *et*
50 *al.*, 2006). ~~To resolve the forcings and feedbacks involved in this transition, multiple nations are targeting recovery of~~
51 ~~continuous ice cores spanning the MPT under the framework of the International Partnerships in Ice Core Science (IPICS)~~
52 ~~oldest ice core challenge (IPICS, 2020).~~

54 ~~The purpose of the current study is to make a simple prediction of atmospheric CO₂ across the MPT. Cross-comparison of~~
55 ~~our and other predicted CO₂ records against observed MPT CO₂ data will aid in testing competing hypotheses on the cause~~
56 ~~of the transition, in particular the role of carbon cycle changes.~~

57
58 The MPT occurred in the absence of any changes to orbital insolation forcing, therefore, the mechanisms behind the MPT
59 must be internal to the earth’s carbon cycle–climate system (Raymo, 1997; Ruddiman *et al.*, 1989). Multiple hypotheses
60 have been put forward to explain the transition. ~~A common element in many of these, is internal climate/earth system~~
61 ~~changes which allow for the development of thicker, more extensive ice sheets that could endure insolation peaks~~

Formatted: Left

Formatted: Font color: Text 1

62 corresponding to the 23 kyr precession and 41 kyr obliquity cycles, i.e., an increase in the threshold for deglaciation and
63 altered sensitivity to orbital forcings (Tzedakis *et al.*, 2017; McClymont *et al.*, 2013). Among the prominent hypotheses are
64 the following three.

65 Three of the more prominent include:

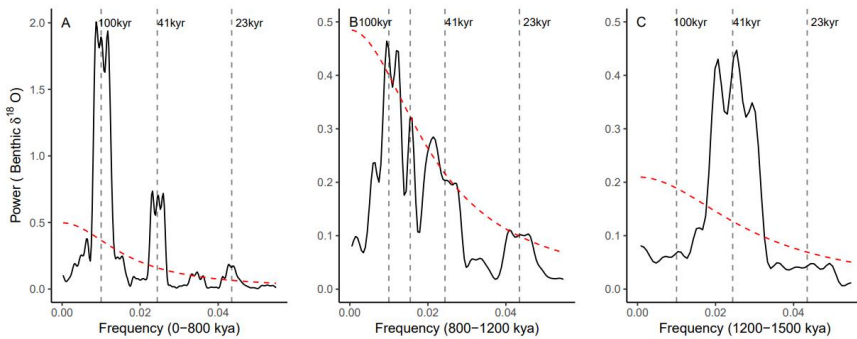
66 1) A long term decrease in radiative forcing, e.g., due to a reduction in atmospheric CO₂ across the transition (e.g., Hönisch *et*
67 *al.*, 2009; Raymo *et al.*, 1988; Berger *et al.*, 1999); 2) Removal of sub-glacial regolith and the subsequent transition from
68 sliding to non-sliding Northern Hemisphere ice sheets (Clark & Pollard, 1998); and 3) Phase-locking of the Northern and
69 Southern Hemisphere ice sheet changes at the orbital precession frequency (Raymo *et al.*, 2006; Raymo & Huybers, 2008).
70 Key to all these hypotheses is a shift toward conditions favorable to building thicker, more persistent, and more globally
71 extensive ice sheets that can skip insolation peaks corresponding to the 23 ky precession and 41 ky obliquity cycles, i.e., an
72 increase in the threshold for deglaciation (Tzedakis *et al.*, 2017).

73 1) A long term decrease in radiative forcing due to a secular reduction in atmospheric CO₂ across the transition (e.g.
74 Berger *et al.*, Hönisch *et al.*, 2009; 1999, Raymo *et al.*, 1988). According to this view, reduced radiative forcing
75 drives the formation of larger and more stable ice sheets.

76 2) Progressive removal of sub-glacial regolith during the 41 kyr glacial cycles. Clark & Pollard (1998) proposed that
77 ice sheet basal sliding prior to the MPT was enhanced by the presence of a low-friction sedimentary regolith layer
78 between the Laurentide ice sheet and the crystalline bedrock. According to this view, progressive removal of this
79 sedimentary layer then favored the development of larger and more persistent post-MPT ice sheets.

80 3) Phase-locking of the Northern and Southern Hemisphere ice sheets. In frequency spectra of the global marine
81 benthic $\delta^{18}\text{O}$ record (Fig. 1) there is no evidence of the precession (23 kyr) component of northern hemisphere
82 insolation prior to the MPT; the spectra is dominated by the obliquity (41 kyr) component (Fig. 1C). Emergence of
83 significant precession and eccentricity signals occurs across the MPT (Fig. 1B), and all three components are
84 clearly present after the MPT (Fig. 1A). Raymo *et al.* (2006) suggested that precession-paced changes in northern
85 and southern hemisphere ice volumes may have occurred prior to the MPT, but are cancelled due to out-of-phase
86 ice volume changes between the two hemispheres (Raymo & Huybers, 2008). According to this view, during the
87 MPT the precession-paced changes to fall into phase between the two hemispheres, such that the precession signal
88 emerges (Raymo *et al.*, 2006). In this view the global synchronization of ice volume drives the formation of larger
89 and more stable ice sheets.

90
91 These hypotheses are not mutually exclusive. For a recent review on the cause of the MPT see Berends *et al.* (2021).



92
93
94 **Figure 1: Thomson Multi-taper Method (MTM) spectral analysis representing relative power of signal periodicity for: A) Benthic**
95 **$\delta^{18}\text{O}$ stack after (0–800 kya) the Mid-Pleistocene Transition (MPT); B) Benthic $\delta^{18}\text{O}$ across the MPT (800–1200 kya); C) Benthic**
96 **$\delta^{18}\text{O}$ prior to the onset of the MPT (1200 kya–1500 kya). Each with a robust AR (1) 95 % Confidence interval (red dashed line).**
97 **Benthic $\delta^{18}\text{O}$ stack data from Lisiecki and Raymo (2005).**

98
99 The key to testing hypotheses on the cause of the MPT is the recovery of a continuous ice core that spans its duration. The
100 International Partnership in Ice Core Sciences (IPICS) has nominated recovery of such a record as a grand challenge in ice
101 core research (IPICS, 2020). Multiple national and international projects have commenced or are soon to commence drilling
102 for ‘oldest ice’. In this project, we take inspiration from the “EPICA Challenge” in which the paleoclimate and modeling
103 community was challenged to predict the global atmospheric carbon dioxide and methane concentrations from 400–800 kya
104 based on the existing 400 ky Vostok ice core record (Wolff *et al.*, 2004). Here, we will use a statistical model on continuous
105 climate archives to predict a CO_2 record for the upcoming 1.5 my ice core and compare these predictions to the discontinuous
106 data available. We utilise two primary data sets: The existing 800 ky ice core composite record of atmospheric CO_2 (Bereiter
107 *et al.*, 2015); and the LR04 benthic stack of 52 globally distributed records of $\delta^{18}\text{O}$ which are a proxy for global ice volume
108 and ocean temperature (Lisiecki & Raymo, 2005). Regression modelling between CO_2 and $\delta^{18}\text{O}$ (sea level and global ice
109 volume proxy) is then used to make predictions of CO_2 spanning 800–1500 kya, spanning the MPT. The regression makes the
110 simple assumption that the relationships between the CO_2 and benthic $\delta^{18}\text{O}$ records can be extended beyond 800 ka; the implicit
111 null hypothesis is that there is no change to the carbon–climate feedback systems outside of the current existing records.

112
113 To test the null hypothesis, we compare our predicted CO_2 record to two sets of low-resolution/imprecisely dated data that
114 exist within the predicted range: 1) CO_2 estimates from the analysis of boron isotope ratios in benthic sediment cores which
115 present a proxy for ocean pH to which a transfer function is applied to reconstruct atmospheric CO_2 (hereafter referred to as

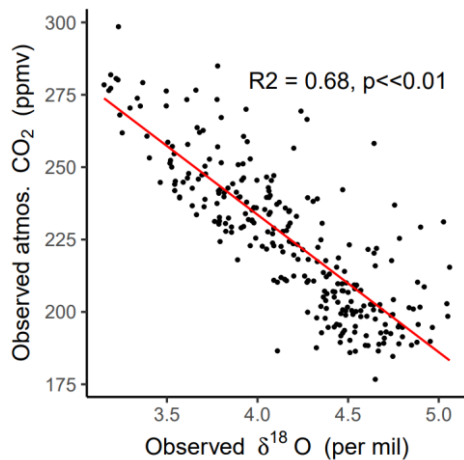
116 BOR-CO₂(Chalk, *et al.*, 2017; Henehan *et al.*, 2013) and 2) direct CO₂ measurements from 1 million year old “blue ice” from
117 the Allan Hills in East Antarctica (hereafter referred to as BI-CO₂) (Higgins *et al.*, 2015). Here we use the term blue ice to
118 describe deep, ancient glacial ice that has been brought to the near surface of an ice sheet by ice flow processes. This makes it
119 some of the oldest, easily accessible ice. However, the vertical migration of the ice is associated with high deformation making
120 the ice samples stratigraphically complex and hard to date (Higgins *et al.*, 2015). As a result, blue ice is not adequate in itself
121 to provide a continuous CO₂ record across the MPT.

122 For a long term decrease in radiative forcing by atmospheric CO₂ to be the cause of the MPT, the reduction in CO₂ would be
123 expected in both glacial and interglacial stages (Chalk *et al.*, 2017). However, low resolution boron-isotope-based CO₂
124 reconstructions by Hönisch *et al.*, (2009), and Chalk *et al.*, (2017) suggest that glacial-stage CO₂ drawdown occurred over
125 the MPT in the absence of interglacial CO₂ drawdown. Glacial-stage CO₂ draw-down across the MPT may be a positive
126 climate-carbon cycle feedback to changes in ice sheet dynamics, including CO₂ drawdown by enhanced iron fertilisation of
127 the Southern Ocean in response to exposed continental shelves due to lower sea level, as well as planetary drying associated
128 with colder climate conditions (Chalk *et al.*, 2017). Colder glacial temperatures that enhance the solubility of CO₂ in the
129 oceans, and reduced abyssal ocean ventilation has also been implicated in enhanced glacial-stage ocean storage of CO₂
130 (McClymont *et al.*, 2013; Hasenfratz *et al.*, 2019).

131
132 Testing of hypotheses on the cause of the MPT is currently limited by the lack of a continuous ice core that spans its
133 duration. The International Partnership in Ice Core Sciences (IPICS) has nominated recovery of such a record as a key
134 priority in ice core research (IPICS, 2020). Multiple national and international projects have commenced, or are soon to
135 commence, drilling for ‘oldest ice’ (see e.g. Shugi, 2022). In this project, we take inspiration from the “EPICA Challenge” in
136 which the paleoclimate and modeling community was challenged to predict the global atmospheric carbon dioxide and
137 methane concentrations from 800–400 kya based on the existing 400 kyr Vostok ice core record (Wolff *et al.*, 2004). Here,
138 we use a generalised least squares (GLS) model trained on continuous climate archives to predict a CO₂ record out to 1.5
139 Mya. We utilise two primary data sets for the GLS model: the existing 800 kyr ice core composite record of atmospheric
140 CO₂ (Bereiter *et al.*, 2015) and the LR04 benthic stack of 52 globally-distributed records of the ¹⁸O to ¹⁶O ratio of fossil
141 benthic foraminifera calcite (hereafter referred to as the LR04 δ¹⁸O benthic stack). The δ¹⁸O ratios in the LR04 benthic stack
142 are governed by ocean temperature and global ice volume at the time the foraminifera lived, with higher values indicating
143 both increased ice volume and a colder climate.

144
145 Fig. 2 shows a scatter-plot of the LR04 δ¹⁸O benthic stack versus observed ice core CO₂ over the past 800 kyr. Both data sets
146 are binned to equivalent 3-kyr time steps (Methods). The Pearson’s correlation coefficient (r) between the data sets is -0.82
147 (p < 0.05) indicating that ~68% of the variance in observed CO₂ is shared with the LR04 δ¹⁸O benthic stack. This strong
148 relationship provides an initial rationale for using the LR04 δ¹⁸O benthic stack as an input parameter to predict CO₂ beyond
149 800 kyr. Mechanistically, multiple processes are expected to contribute to the shared variance. A first order factor is the

150 [dependency of CO₂ solubility on ocean temperature \(e.g. Millero, 1995\)](#). From the simple solubility perspective, colder
151 [climate states with increased ice volume and colder ocean temperatures will drive increased ocean uptake of CO₂ \(Berends *et al.*, 2021\)](#). However, the solubility effect only accounts for a portion of observed glacial CO₂ drawdown (Archer *et al.*,
152 [2000](#)). Multiple additional contributors to the shared variance are proposed in the literature. These include (not
153 [exhaustively](#)), direct radiative forcing of ice volume changes by CO₂ (e.g. Shackleton *et al.*, 1985); the impact of ice
154 [volume/sea level changes on atmospheric CO₂ via ocean productivity and carbonate chemistry changes \(e.g. Broecker, 1982;](#)
155 [Archer *et al.*, 2000; Ushie and Matsumoto, 2012\); CO₂ drawdown during periods of high ice volume by increased iron](#)
156 [fertilization \(e.g. Rothlisberger *et al.*, 2004; Martinez-Garcia *et al.*, 2014\) and enhanced sea ice extent during periods of high](#)
157 [ice volume capping the ventilation of CO₂ from the ocean interior at high latitudes \(Stephens and Keeling, 2000\)](#).
158
159
160 [A quantitative separation and attribution of the processes linking global ice volume, ocean temperature and atmospheric CO₂](#)
161 [on millennial to orbital timescales is not currently available \(e.g. Archer *et al.*, 2000; Sigman *et al.*, 2010; Gottschalk *et al.*,](#)
162 [2019\) and will not be attempted here. Rather, we make the simple assumption that the relationships between the LR04](#)
163 [benthic δ¹⁸O stack and CO₂ can be extended beyond 800 kya and use regression modelling between benthic δ¹⁸O and CO₂ to](#)
164 [make a predictions of CO₂ spanning 800–1500 kya. The deliberately simple implicit assumption, and null hypothesis, is that](#)
165 [there is no change to the feedback processes linking benthic δ¹⁸O and CO₂ before and after the MPT](#).
166



167 **Figure 2: Scatter plot of the composite observed atmospheric CO₂ record (Bereiter *et al.*, 2015) against the LR04**
168 **benthic stack of marine δ¹⁸O records (Lisiecki & Ravmo, 2005). Red line is a linear line of best fit ($R^2 = 0.68$; $p <$**
169 **0.05).**

170
171
172 To test the null hypothesis, in advance of the recovery of a continuous ice core, we compare our predicted CO₂ record to two
173 sets of low-resolution ice core data that exist outside the current 800 kyr observed CO₂. These data come from direct CO₂
174 measurements from ancient “blue ice” from the Allan Hills in East Antarctica (hereafter referred to as BI-CO₂) from ca. 1
175 Mya (Higgins *et al.*, 2015) and 1.5 Mya (Yan *et al.*, 2022). We use the term blue ice to describe deep, ancient glacial ice that
176 has been brought nearer to the surface of an ice sheet by ice flow. Blue ice is sampled by cutting trenches or shallow drilling
177 of up to several hundred meters (e.g. Higgins *et al.*, 2015). The vertical migration of blue ice is associated with high
178 deformation making the ice samples stratigraphically complex and hard to date (Higgins *et al.*, 2015). As a result, blue ice
179 records alone do not provide a continuous CO₂ record across the MPT. We also compare our predicted record to existing
180 proxy-CO₂ reconstructions from boron-isotope analysis of benthic foraminifera in marine sediment records (Chalk, *et al.*,
181 2017; Dyez *et al.*, 2018; Guillermic *et al.*, 2022), leaf wax δ¹³C carbon isotope ratios (Yamamoto *et al.*, 2022) and
182 predictions from previous models of various complexities (van de Wal *et al.*, 2011; Willeit *et al.* 2019). We conclude with
183 discussion of the implications of our results and data-comparisons for the understanding MPT dynamics.
184

185 2 Methods

186 ~~We calculated the mean of the Bereiter *et al.*, (2015) CO₂ record at 3 ky resolution time bins. To obtain constant resolution~~
187 ~~between the predictor and response variables to run the model, we also binned the LR04 Benthic Stack to this resolution. To~~
188 ~~account for autocorrelation in the data, which would lead in inaccurate predictions in an ordinary least squares model, we~~
189 ~~utilized generalized least squares (GLS) regression models with a correlation factor for the model. The factor used yielded the~~
190 ~~lowest Akaike information criterion (AIC) value from a test of multiple correlation factors. Ultimately, we chose an AR(1)~~
191 ~~correlation factor for the model. The GLS regression model was performed over the 0–800 ky range of the predictor variable~~
192 ~~(LR04 Benthic Stack) and the response variable (CO₂). Based on the regression model the δ¹⁸O values of the LR04 Benthic~~
193 ~~Stack from 800–1500 kya were used to predict CO₂ concentration over this range (hereafter referred to as PRED-CO₂). We~~
194 ~~took a bootstrap approach, selecting a random 50% subset of our data and running the model 1000 times to determine 95%~~
195 ~~confidence intervals for the predictions. Finally, we compared our PRED-CO₂ record to some sparse and discrete data that~~
196 ~~exists outside of the current continuous ice core data from 800–1500 kya.~~

197 We use a generalised least squares (GLS) model to predict atmospheric CO₂ from the LR04 benthic δ¹⁸O stack (Fig. 3A and
198 B). We apply an AR(1) correlation factor to account for autocorrelation in the data. The AR(1) correlation factor yielded the
199 lowest Akaike information criterion (AIC) value from a test of multiple correlation factors. To obtain common time steps
200 and resolution between the predictor (LR04 benthic δ¹⁸O stack) and response (CO₂) variables, we re-grid the LR04 benthic

201 stack and Bereiter *et al.*, (2015) CO₂ data into time bins with a resolution of 3-kyr. The GLS regression model was applied
202 over the 0–800 kyr range of the predictor and response variables as follows:

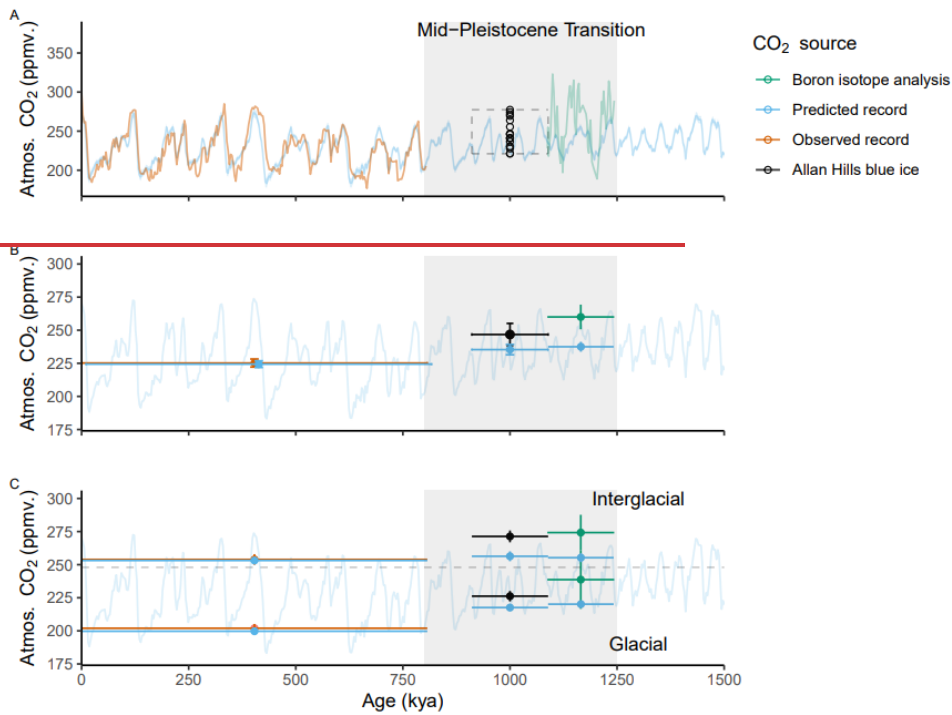
$$CO_2 = 33.37 \times \delta^{18}O + 365.15, \text{ autoregressive (AR) factor: } 1$$

206 Based on the regression model, the $\delta^{18}O$ values of the LR04 Benthic Stack from 800 – 1500 kya were used to predict CO₂
207 concentration over this range (hereafter referred to as PRED-CO₂). To estimate the GLS model uncertainty and sensitivity
208 we took a bootstrap approach, selecting a random 50% subset of our data and re-running the model 1000 times to determine
209 95% confidence intervals for the predictions.

211 Uncertainties in the independent age scales of both the LR04 stack and the compiled CO₂ record are inherited by our GLS
212 model and its predictions. The LR04 stack includes 57 globally-distributed benthic $\delta^{18}O$ sediment core records. The age
213 models for these cores are independently constructed from the average sedimentation rates of each core, assuming global
214 sedimentation rates have remained relatively stable, and with tuning to a simple ice model based on 21 June insolation at
215 65°N (Lisiecki & Raymo, 2005). The authors estimate uncertainty of 6 kyr from 1.5 – 1.0 Mya and 4 kyr from 1 – 0 Mya
216 (Lisiecki & Raymo, 2005). The observed CO₂ composite ice core record for the past 800 kya (Bereiter *et al.*, 2015) uses six
217 independent dating methods for various core locations both spatially across Antarctica, and stratigraphically for different
218 sections of the same core. The age uncertainty in the gas timescale has a median over the 0 – 800 kya interval of 2 kyr, but
219 individual uncertainties can reach up to 5 kyr (Veres *et al* 2013; Bazin *et al.*, 2013). The relative age uncertainties between
220 these input variables may diminish the regression or in some instances lead to spurious correlation. However, we expect any
221 such effects are minor on the basis that our predictions show little sensitivity to the bootstrap analysis with 1000 iterations of
222 re-computing the regression after removing 50% of data (see Fig. 3B, C and Discussion).

224 **3 Results**

225 Our model skillfully predicts atmospheric CO₂ over the past 800 ky (Fig. 1A) ($r(226) = .86$, $p = \ll 0.01$). However, across the
226 MPT the PRED-CO₂ data is systematically lower when averaged over its common intervals with the Allan Hills BI CO₂ and
227 BOR CO₂ beyond 800 kya (Fig. 1B). The average BI CO₂ concentration (at 1000 ± 89 kya) is ~ 11 ppm higher than our
228 predicted value (averaged over the age uncertainty of the BI-CO₂) and the 95% confidence interval (1.96σ) overlap by 0.88
229 ppm; see blue and black bars in Fig. 1B). Similarly, the average BOR CO₂ data from the early MPT (ca. $\sim 1.1 - 1.15$ mya) is ~ 22
230 ppm higher than our predicted value (green and blue bars in Fig. 1B). Our model appears to underpredict CO₂ increasingly
231 with time, although the rate of this change may not be uniform.



232
 233 **Figure 1: A) Comparison of our PRED-CO₂ (ppm) record to the current continuous composite record; CO₂ estimates**
 234 **from boron isotope analysis of benthic foraminifera shells (BOR-CO₂) (Chalk, et al., 2017), and direct CO₂**
 235 **measurements from Allan Hills blue ice core data (BI-CO₂) (Higgins et al., 2015). Indicators for age uncertainty**
 236 **boundaries (± 89 ky) of the blue ice represented by dashed boundaries. B) The mean CO₂ concentration of the predicted**
 237 **record over the range of the observed composite record (offset for clarity) and the age uncertainty range of the BI-CO₂**
 238 **data; mean concentrations of the observed composite CO₂ record; mean concentration of BI-CO₂ over its age**
 239 **uncertainty range; and the average BOR-CO₂ concentration. C) The same as B) but filtered by the highest and lowest**
 240 **25th percentile of $\delta^{18}\text{O}$ to represent glacial and interglacial periods; but BI-CO₂ data filtered by highest and lowest**
 241 **25th percentile of CO₂.**

242
 243 We define the interglacial and glacial thresholds of CO₂ to be the top and bottom 25th percentile of the $\delta^{18}\text{O}$ signal, respectively
 244 (following Chalk *et al.*, 2017). Applying this filtering to the predicted record and the observed composite CO₂ record for the

245 post-MPT (0–800 kya) interval demonstrates a close match (Fig. 1C). Applying the same filtering to our predicted record
246 across the MPT (800–1500 kya) indicates a significant lowering of glacial-stage CO₂ concentration; while no significant change
247 in the interglacial-stage CO₂ concentration was detected (ANOVA, $F_{1,52} = 25.49, p = 4.86e^{-06}$; ANOVA, $F_{1,57} = 1.47, p = 0.23$
248 respectively). As a change in radiative forcing (ARF) is a direct conversion of CO₂ concentration (IPCC, 2001), the PRED-
249 CO₂ data would translate to a significant decline in ΔRF in glacial, but not interglacial stages across the MPT (as was suggested
250 by Chalk *et al.*, 2007; Hönisch *et al.*, 2009).

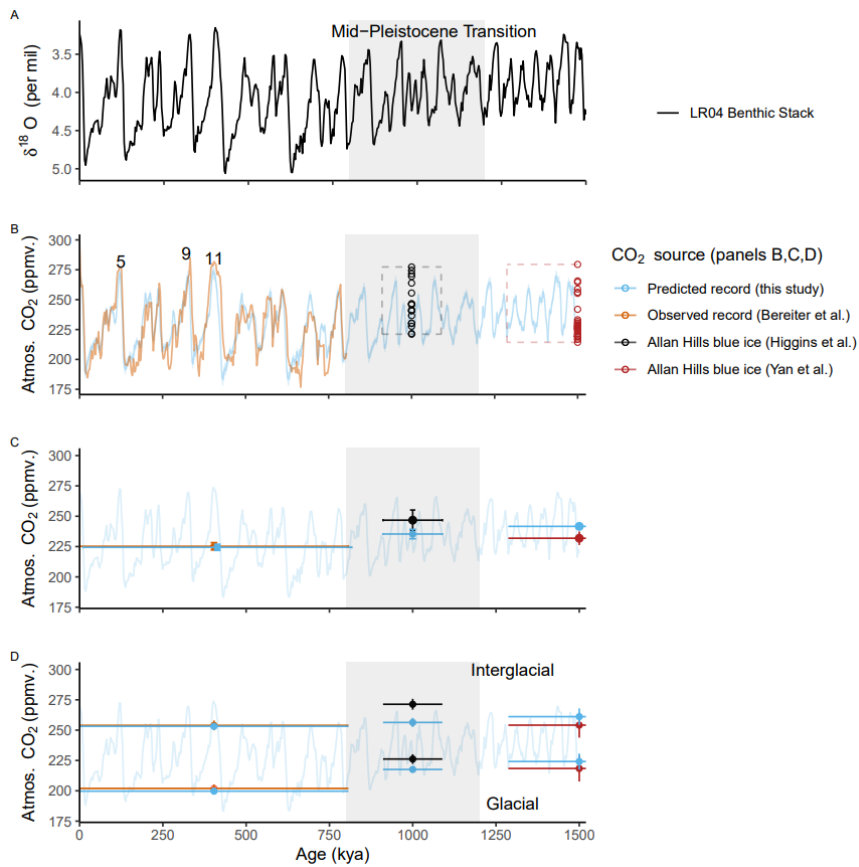
251
252 Filtering BOR-CO₂ and BI-CO₂ by the same definition and averaging over their respective range ($\delta^{18}\text{O}$ linearly interpolated
253 for BOR-CO₂ data) indicates that the model underpredicts relative to both the BI-CO₂ and BOR-CO₂ data for both glacial and
254 interglacial stages during the MPT interval (800–1250 kya) (Fig. 1C). Overall, we see increasing difference between our
255 predicted data and the sparse estimates over the MPT (BOR-CO₂ and BI-CO₂) going further back in time.

256
257 Various studies conclude that glacial-stage draw-down of CO₂ occurs across the MPT in the absence of interglacial draw-down
258 (e.g., Chalk *et al.*, 2017; Hönisch *et al.*, 2009). This trend is seen in our predicted record, and in the filtered BI-CO₂ and BOR-
259 CO₂ data (Fig. 1C). Importantly, the periodicity is consistent between our predicted record and the BOR-CO₂ data (i.e., the
260 glacial and interglacial peaks and troughs coincide). Hence, the BOR-CO₂ and BI-CO₂ challenge the amplitude but not the
261 periodicity of our predicted data. These results support rejection of our null hypothesis and provide quantitative evidence of a
262 fundamental change in the carbon–climate feedback system having occurred across the Mid-Pleistocene Transition.

263 Fig. 3B shows the time series of our LR04 benthic $\delta^{18}\text{O}$ stack-based GLS model predictions of atmospheric CO₂ (PRED-
264 CO₂) over the past 800 kyr, in comparison to the observed ice core CO₂ record from Bereiter *et al.*, (2015). The correlation
265 coefficient (r^2) between the predicted and observed records is 0.68 ($p \ll 0.01$). Our PRED-CO₂ record out to 1.5 Mya is also
266 shown, overlain with observed Allan Hills blue ice CO₂ (BI-CO₂) datasets of age 1000 ± 89 kya (Higgins *et al.*, 2015) and
267 $1.5 \text{ Mya} \pm 213$ kyr (Yan *et al.*, 2022).

268
269 We evaluate the PRED-CO₂ record against the observed CO₂ data according to criteria of mean concentrations across the
270 common intervals, and mean concentrations in the glacial and interglacial subsets of the data. First, the mean CO₂
271 concentration over the common intervals (Fig 3C). From 0–800 kya the mean concentration in observed (Bereiter *et al.*,
272 2015) and PRED-CO₂ data are in close agreement (225.2 ± 3.03 ppm versus the predicted 225.1 ± 2.5 ppm respectively;
273 uncertainties are 95% confidence intervals, i.e. 1.96σ). In the 1000 ± 89 kya interval (i.e. averaged across the age uncertainty
274 of the Higgins (2015) blue ice data) the BI-CO₂ concentration is ~ 11 ppm higher than PRED-CO₂ (246.7 ± 8.4 ppm versus
275 the predicted 235.5 ± 3.9 ppm), this difference is not significant at the 95% confidence level. For the $1.5 \text{ Mya} \pm 213$ kyr
276 interval, the mean BI-CO₂ concentration is ~ 10 ppm lower than PRED-CO₂ (231.9 ± 5.6 ppm versus the predicted $241.7 \pm$
277 2.5 ppm), which is marginally significant at the 95% level. Comparisons of mean levels across intervals spanning multiple

278 glacial and interglacial cycles may be biased if (as is likely) the blue ice data is not sampling glacial and interglacial values
279 with the same uniformity as a continuous record.
280
281 To address this, we define the glacial and interglacial thresholds of PRED-CO₂ to be respectively the lower and upper 25th
282 percentiles of the LR04 δ¹⁸O predictor variable (following Chalk *et al.*, 2017). Filtering the observed (Bereiter *et al.*, 2015)
283 CO₂ record and our predicted CO₂ record according to these definitions we find a very close match for glacial (202.0 ± 3.2
284 versus the predicted 199.7 ± 1.7 ppm) and interglacial intervals (253.9 ± 4.1 ppm versus the predicted 253.1 ± 2.3 ppm), over
285 the past 800 kya (see Fig. 3D). For blue ice (BI- CO₂) data, a corresponding LR04 isotope signal could not be confidently
286 applied to the measured CO₂ concentration due to the uncertainties associated with blue ice aging; therefore, we defined the
287 glacial and interglacial thresholds of blue ice data according to the top (interglacial) and bottom (glacial) 25th percentiles of
288 actual CO₂. Applying this to the 1000 ± 89 kya interval finds that observed BI-CO₂ data is ~ 9 ppm higher than PRED-CO₂
289 during the glacial stages (226.2 ± 4.0 ppm versus the predicted 217.6 ± 2.3 ppm) and ~ 15 ppm higher than PRED-CO₂
290 during the interglacial stages (271.3 ± 4.5 versus the predicted 256.3 ± 3.8 ppm). These differences are significant with
291 respect to the constrained uncertainties. In contrast, during the 1.5 Mya ± 213 kyr interval, the mean BI- CO₂ concentration
292 is not significantly different to PRED-CO₂ in either glacial (217.6 ± 2.3 versus the predicted 224.2 ± 6.6 ppm) or interglacial
293 stages (256.3 ± 3.8 versus the predicted 261.1 ± 6.3 ppm). These comparisons, particularly the agreement at 1.5 Myr,
294 indicate that PRED-CO₂ is not drifting systematically away from the existing observed BI-CO₂ data. In our view the
295 disagreement at 1.0 Myr, where BI-CO₂ is elevated with respect to PRED-CO₂, does not give sufficient cause to reject the
296 GLS model, it could of course be a failing in the model and/or could be due to potential biases in the blue ice data, for
297 example elevated CO₂ concentrations due to in-situ CO₂ production in blue ice (see Discussion).



298
 299 **Figure 3: A) The LR04 Benthic Stack of 57 globally distributed $\delta^{18}\text{O}$ records (Lisiecki & Raymo, 2005). B)**
 300 **Comparison of our PRED- CO_2 (ppm) record to the current continuous composite record (0–800 kya); and to direct**
 301 **CO_2 measurements from Allan Hills blue ice cores (BI- CO_2) ca. 1 Mya (± 89 kyr) (Higgins *et al.*, 2015) and ca. 1.5**
 302 **Mya (± 213 kyr) (Yan *et al.*, 2022). Age uncertainty boundaries for the BI- CO_2 data are represented by dashed box**
 303 **boundaries. Marine isotope stages 5, 9, and 11 are numbered on the plot according to Lisiecki & Raymo (2005). C)**
 304 **Mean concentrations of the PRED- CO_2 and observed composite CO_2 records over the range of the observed**
 305 **composite record (offset for clarity), and the mean concentrations of the PRED- CO_2 and BI- CO_2 data at 1 Mya and**

306 again at 1.5 Mya averaged over the age uncertainty range of each BI-CO₂ data set. D) As for C) however filtered by
307 the upper and lower 25th and 75th percentiles to estimate glacial and interglacial periods.

308
309 We now consider long-term trends in interglacial and (separately) glacial CO₂ levels across the past 1.5 Myr in PRED-CO₂
310 and in the existing ice core CO₂ data. For PRED-CO₂ there is no significant difference between CO₂ concentrations in the
311 interglacial stages of the 1.5 Mya ± 213 kya, 1000 ± 89 kya and 0–800 kya windows (Fig 4 D, blue bars). In the ice core
312 observations, interglacial levels at 1.5 Mya in BI-CO₂ are also within the uncertainties of those in the 0–800 kya interval.
313 Notably, the BI-CO₂ concentrations in the 1000 ± 89 kya interval appear elevated with respect to the 0–800 kyr and 1.5 Mya
314 ± 213 kya intervals, however this elevated (ca. 271 ppm) level is consistent with the observed interglacial CO₂ concentration
315 during interglacials 5, 9 and 11 (Fig 3B). Overall, there is no indication in the observed ice core CO₂ data or in PRED-CO₂
316 for a long-term trend in interglacial CO₂ levels across the past 1.5 Myr.

317
318 In comparison, there are significant declines in glacial CO₂ levels across the MPT in PRED-CO₂ and the observed ice core
319 data. For PRED-CO₂, glacial CO₂ concentrations are not significantly different during the 1.5 Mya ± 213 kya and 1000 ± 89
320 kya windows. However, across the MPT, PRED-CO₂ glacial concentrations drop by ~18 ppm. This pattern is consistent with
321 the observed data, where glacial CO₂ levels are also not significantly different between the 1.5 Mya ± 213 kya and 1000 ± 89
322 kya windows (217.6 ± 2.3 and 226.2 ± 4.0 ppm, respectively) and then fall by 24 ppm to the 0–800 kyr observed glacial
323 mean of 202.0 ± 3.2 ppm. Glacial-stage draw-down of CO₂ across the MPT in the absence of interglacial draw-down is
324 consistent with previous observations based on the boron-isotope-based CO₂ reconstructions (e.g., Chalk *et al.*, 2017;
325 Hönisch *et al.*, 2009 and see Discussion). In the following section we also compare PRED-CO₂ data to boron-isotope-based
326 and other CO₂ proxy records covering the 0 to 1.5 Myr interval.

328 **4 Discussion**

329 In 2004, the community of Earth System modelers were issued a challenge: to predict what an 800 ky carbon dioxide record
330 may look like prior to the final analysis of the EPICA Dome C (EDC) ice core (Wolff *et al.*, 2004). Here we have adapted the
331 EPICA Challenge to examine the MPT problem of the currently unknown mechanisms behind the transition from the 41 ky to
332 100 ky glacial cycle. However, unlike the EPICA challenge, we had the opportunity to compare our predictions to discrete
333 data outside of the range of the continuous training data sets prior to the recovery of a continuous ice core spanning the MPT.
334 These data were direct CO₂ measurements from ~1 my old blue ice, and CO₂ estimates from the analysis of boron ratios in
335 deep sea sediments (ca. ~1.1–1.25 mya). This has allowed us to preemptively examine differences in climate responses over
336 the last 1.5 my. We now consider the implications of our results for hypotheses on the cause of the MPT.

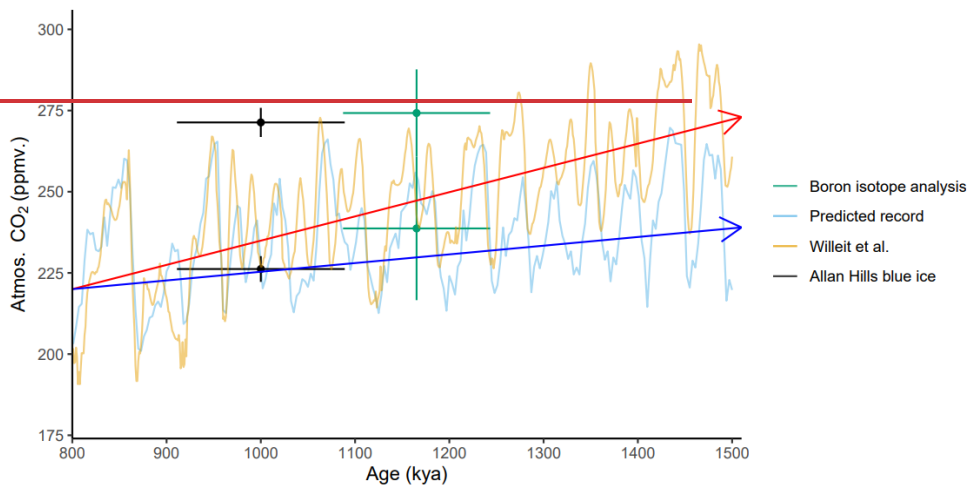
4.1 Predicted changes to the climate-carbon cycle-cryosphere feedback system

The BOR-CO₂ and BI-CO₂ data supports the conclusion that an increase in the glacial to interglacial CO₂ difference has occurred across the MPT and that this difference is dominated by glacial stage CO₂ drawdown. We estimate the CO₂ glacial to interglacial difference has increased from -36 ppm in the early MPT (ca. -1.1-1.25 mya, BOR-CO₂) to -52 ppm (observed composite CO₂ record) after the MPT (0-800 kya). Our PRED-CO₂ record also presents significant glacial stage reduction over the MPT, although to a lesser extent than BOR/BI-CO₂ (FIG. 1C). The reduction in only glacial stage CO₂ across the MPT is inconsistent with the theory that a long term decline in radiative forcing exerted by CO₂ (in both glacial and interglacial stages) was the main cause of the climate transition from the 40 ky world to the 100 ky world. This conclusion is consistent with results from Chalk *et al.* (2017) and Hönisch *et al.*, (2009) who associate the glacial stage CO₂ draw down to a change in the global carbon cycle across the MPT.

Glacial stage CO₂ draw down across the MPT may itself be a positive climate-carbon cycle-cryosphere feedback response to changes in ice sheet dynamics that favours enhanced glacial persistence over time (Chalk *et al.*, 2017). Potential processes allowing for the stabilization and persistence of ice sheets include the removal of sub-glacial regolith (Clark & Pollard, 1998), or Northern and Southern Hemisphere phase locking (Raymo *et al.* 2006; Raymo & Huybers, 2008). Either (or both) processes could allow for the persistence of ice sheets through obliquity (and potentially precession) dominated orbital cycles, i.e., a gradual rise in the threshold for deglaciation (Tzedakis *et al.*, 2017). This persistence would promote glacial stage CO₂ decline, potentially through iron fertilisation of the Southern Ocean in response to increased ice volume and the planetary drying associated with colder climate conditions (Chalk *et al.*, 2017). In turn, further glacial stage build up of ice sheets would be favoured by the reduced radiative forcing (Chalk *et al.*, 2017). Colder glacial temperatures that enhance the solubility of CO₂ in the oceans, and changes to ocean circulation have also been implicated in enhanced ocean storage of glacial stage CO₂ (Hasenfratz *et al.*, 2019). Furthermore, relative sea level (SL) changes in the Mediterranean Sea (derived from a reconstruction through local benthic δ¹⁸O) (Rohling *et al.*, 2014) between the early MPT and late Pleistocene reveal increased sensitivity to radiative forcing. That is, 1 W m⁻² reduction in radiative forcing (RF) by CO₂ results in a more pronounced lowering of SL in the late Pleistocene than at the early MPT (Chalk *et al.*, 2017).

The clear offset between our PRED-CO₂ data and the sparse data pre dating this record provides further evidence of a fundamental shift in the climate-carbon cycle-cryosphere feedbacks across the MPT. However, BOR-CO₂ and BI-CO₂ both have large concentration and timing uncertainties respectively, so the definitive test awaits a continuous ice core across the MPT. One modelling study that captures enhanced atmospheric CO₂ draw down during glacial stages across the MPT is that of Willeit *et al.*, (2019). These investigators reconstructed atmospheric CO₂ over the past three million years under a regolith removal scenario, which can be compared to our modelled data (Fig. 2). Note the increasing difference with time between our predicted CO₂ level and that of Willeit *et al.*, (2019). Our simple model underpredicts CO₂ levels compared to the sparse

370 observations (BOR/BI- CO_2) and Willeit *et al.*, (2019). The implication is that additional physics, not captured in our LR04 stack-
 371 based predictions, is required to explain the divergence. These additional physics could include the gradual removal of sub-
 372 glacial regolith, allowing for increased “stickiness” of Northern Hemisphere ice sheets (as described by Clark and Pollard
 373 (1998), and the scenario for the model by Willeit *et al.*, (2019)); and/or the phase locking of the Northern and Southern
 374 Hemisphere ice sheets at the precession frequency due to a transition to marine-based ice sheet margins in Antarctica (as
 375 described by Raymo *et al.*, (2006)). Both scenarios would have enabled the northern hemisphere ice sheets to persist past the
 376 obliquity-paced threshold for deglaciation prior to the onset of the MPT.



377
 378 **Figure 2: The modelled CO_2 record of Willeit *et al.*, (2019) overlayed on our predicted CO_2 record across and beyond**
 379 **the MPT (800—1500 kya). Arrows represent the trajectory of atmospheric CO_2 under two conditions: 1) CO_2**
 380 **reconstructed under our null hypothesis that no change to the carbon—climate feedback system has occurred before**
 381 **and across the MPT (blue). 2) The trajectory of atmospheric CO_2 that more accurately represents the discrete**
 382 **measurements/estimates we have across the MPT (red).**

383 4.2 Our model with respect to the phase-locking hypothesis

384 The predicted CO_2 record presented in this study cannot decisively test the phase locking hypothesis for the MPT until
 385 continuous oldest ice records have been recovered. Being entirely based on the LR04 Benthic Stack, our predictions inherit all
 386 the observed power spectra in the training data (Fig. A). Our predictions also inherit the climate—carbon cycle—cryosphere
 387 relationships over the past 800 ky during which time the Northern and Southern Hemisphere ice sheets have been in phase
 388 with each other on orbital timescales (Raymo *et al.*, 2006). For this reason, differences between the observed oldest ice records

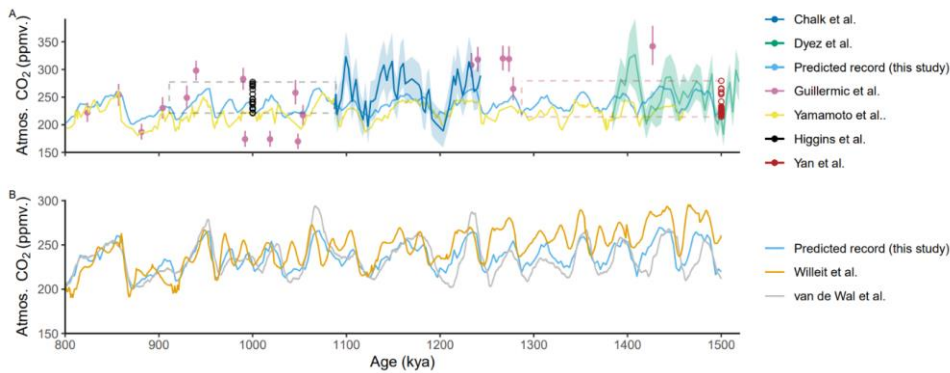
389 ~~and our predicted data will shed light on the phase locking hypothesis. If the Northern and Southern hemisphere ice sheets did~~
390 ~~vary out of phase in the “40 kyr world” then we would expect to see large discrepancies between the PRED CO₂ record~~
391 ~~presented here and the realised data.~~

393 Our objective with this manuscript was to generate the simplest reasonable model to predict CO₂ from the LR04 δ¹⁸O
394 benthic stack and to test the predictions against available observations. It is possible that the fit between observed and our
395 predicted CO₂ data could be further improved using a non-linear approach. However, we refrain from a non-linear approach
396 for several key reasons. First, a scatter plot of the LR04 δ¹⁸O benthic stack versus observed ice core CO₂ over the past 800
397 kyr yields a Pearson’s correlation coefficient (R) of -0.82 (Fig. 2), indicating that ~68% of the variance in observed CO₂ is
398 shared with the benthic stack. Importantly, there is no evidence in this scatter plot for departure from the linear relationship
399 at high or low CO₂ or benthic δ¹⁸O levels. Second, following the approach of Chalk *et al.*, 2017 and interpreting the upper
400 25th percentile of CO₂ data as representing mean interglacial stage CO₂ and the lower 25th percentile of CO₂ data as
401 representing mean glacial stages CO₂ levels, we see that our predicted interglacial mean value for the past 800 kyr (253.1 ±
402 2.3 ppm) closely overlaps with the observed interglacial mean value (253.9 ± 4.1 ppm) and similarly, the predicted glacial
403 stage mean (199.7 ± 1.7 ppm) closely overlaps with the observed glacial stage mean (202.0 ± 3.2 ppm). Third, the
404 predictions are remarkably insensitive to bootstrap analysis in which 50 % of that data are omitted with each iteration of the
405 GLS model (Fig 1). Such insensitivity to the bootstrap analysis and accurate prediction of glacial *and* interglacial state CO₂
406 values would be unlikely in the case of major non-linear dependencies between the LR04 predictor and CO₂ response
407 variables. Fourth, non-linear approaches would risk generating an improved fit due to statistical artefacts that do not
408 meaningfully relate to any dependence between benthic δ¹⁸O and CO₂. Finally, the specific causes and sources and sinks
409 involved in glacial to interglacial and millennial-scale CO₂ variations still remain poorly constrained (e.g. Archer *et al.*,
410 2000; Sigman *et al.*, 2010; Gottschalk *et al.*, 2019). Given this process-uncertainty, the GLS model fits our criteria of the
411 simplest reasonable model. Further, the use of benthic δ¹⁸O to predict atmospheric CO₂ has precedence; in response to the
412 EPICA challenge (Wolff *et al.*, 2004), N. Shackleton used this method to predict atmospheric CO₂ out to 800 kyr (Wolff,
413 2005). Furthermore, inverse modelling of CO₂ forced by the LR04 benthic stack has been undertaken by Berends *et al.*
414 (2021a) and van de Wal *et al.* (2011).

415
416 There are several caveats with blue ice data that may affect its use to evaluate our GLS model predictions. The blue ice data
417 may have been subject to diffusional smoothing of CO₂ (e.g. Yan *et al.*, 2019), which would act in the direction of elevating
418 the (lower 25th percentile) assumed glacial concentrations above the glacial atmospheric values and reducing the (upper 25th
419 percentile) assumed interglacial concentrations. There is also the potential for artificially elevated CO₂ concentrations in blue
420 ice due in-situ respiration of CO₂ due to microbial activity in detrital matter. Respiration effects are screened for by
421 measurements of δ¹³C of CO₂, however it is difficult to demonstrate that all samples are unaffected (Yan *et al.*, 2019). These
422 uncertainties support our argument that the GLS-model predictions are not rejected by the available observed BI-CO₂ data.

423
424 We consider the BI-CO₂ data to provide the most reliable measurements of CO₂ concentration, in the absence of a
425 continuous ice core record across the MPT. However, further comparison of our CO₂ predictions can also be made against
426 CO₂ proxy data from non-ice core archives (Fig 4A). We consider here $\delta^{11}\text{B}$ -based atmospheric CO₂ reconstructions (Chalk
427 *et al.*, 2017, Dyez *et al.* 2018 and Guillermic *et al.* 2022) and a recent atmospheric CO₂ reconstruction from $\delta^{13}\text{C}$ of leaf wax
428 (Yamamoto *et al.*, 2022). The continuous $\delta^{11}\text{B}$ -based reconstructions of Dyez *et al.*, (2018) overlap PRED-CO₂ from ~1.38 –
429 1.5 Mya while the Chalk *et al.*, (2017) reconstruction overlaps PRED-CO₂ from 1.09 – 1.43 Mya. Discrete reconstructions
430 from Guillermic *et al.* (2022) are distributed non-uniformly across the 800 to 1.5 Mya interval. For the two continuous $\delta^{11}\text{B}$ -
431 based reconstructions (Chalk *et al.*, (2017) and Dyez *et al.*, (2018)) the glacial CO₂ levels appear consistent with the PRED-
432 CO₂ record, within their reported 30 – 60 ppm uncertainties. However, $\delta^{11}\text{B}$ -based interglacial stages in these reconstructions
433 exceed those of the PRED-CO₂ record (Fig. 4A). The Guillermic *et al.* (2022) reconstructions suggest a larger range of CO₂
434 concentrations than the overlapping intervals of PRED-CO₂ and of the two continuous $\delta^{11}\text{B}$ -based reconstructions (Fig. 4A).
435 The large range of the Guillermic *et al.* (2022) data and the high interglacial maxima in the Chalk *et al.* (2017) and Dyez *et*
436 *al.*, (2018) data, all significantly exceed the range and interglacial maxima from the BI-CO₂ estimates. These discrepancies
437 internally between different $\delta^{11}\text{B}$ -based CO₂ reconstructions and between the $\delta^{11}\text{B}$ -based reconstructions and the BI-CO₂
438 data, may be due to uncertainties associated with the $\delta^{11}\text{B}$ proxy transfer function. The $\delta^{11}\text{B}$ -based CO₂ reconstructions are
439 dependent on assumptions about multiple components of the carbonate system, including local marine carbon chemistry and
440 the CO₂ saturation state in the past and (Hönisch *et al.*, 2009). Evidence that $\delta^{11}\text{B}$ -based reconstructions may overestimate
441 interglacial stage CO₂ is also seen in data from Chalk *et al.*, (2017) spanning ca. 0–250 kya, where the $\delta^{11}\text{B}$ -based
442 interglacial CO₂ levels exceed the continuous ice core CO₂ record by ca. 30 ppm (not shown).
443
444 By comparison, the $\delta^{13}\text{C}$ of leaf wax data (Yamamoto *et al.*, 2022) has a similar glacial to interglacial range as PRED-CO₂,
445 but a ca. 20ppm lower mean concentration than our predictions (Fig 4A). Hence, our PRED-CO₂ data fall lower than
446 interglacial $\delta^{11}\text{B}$ -based interglacial levels but are higher than the $\delta^{13}\text{C}$ of leaf-wax based estimate. Given the evidence that
447 $\delta^{11}\text{B}$ -based reconstructions are known to overestimate atmospheric CO₂ concentration in the continuous ice core record, we
448 do not find cause from the existing CO₂ proxy data to reject our predictions nor our associated null-hypothesis.
449
450 We also compare our predictions to existing more complex model simulations (Fig 4B.). First, against a transient simulation
451 using an intermediate-complexity earth system model (CLIMBER-2) by Willeit *et al.* (2019). This study suggests a
452 combination of gradual regolith removal and atmospheric CO₂ decline can explain the long-term climate variability over the
453 past 3Myr. Second, against a longer-term reconstruction by van de Wal *et al.* (2011) that utilises deep-sea benthic isotope
454 records to reconstruct a continuous CO₂ record over the past 20 Myr. Our simple GLS model demonstrates a similar long-
455 term trend and timing of glacial-interglacial signals and an atmospheric CO₂ level that sits approximately mid-way between
456 the two more complex models.

457



458

Figure 4: A) Predicted CO₂ (this work) compared to observed, proxy CO₂ estimates from a range of other sources: $\delta^{11}\text{B}$ -based pCO₂ reconstructions and measurements by Dyez *et al.* (2018), Guillermic *et al.* (2022); Chalk *et al.* (2017); blue ice CO₂ measurements by Yan *et al.* (2019) and Higgins *et al.* (2015); $\delta^{13}\text{C}$ leaf wax proxy reconstructions by Yamamoto *et al.* (2022). The dashed boxes indicate the dating uncertainty and range of the respective BI-CO₂ records. B) Our predicted record compared to various model simulations: a regolith removal hypothesis simulation by Willeit *et al.* (2019); and a high-resolution CO₂ reconstruction by van de Wal *et al.* (2011)

465

A complete and critical test of our and other CO₂ predictions awaits the upcoming analysis of the continuous oldest ice core records. We now discuss some potential applications of the PRED-CO₂ record for hypothesis testing on the cause of the MPT.

469

PRED-CO₂ shows a long-term decline in glacial CO₂ across the MPT, but no long-term decrease in interglacial CO₂. This pattern is consistent with the boron-isotope-based CO₂ reconstructions shown earlier, where it is often described as an increase in the interglacial to glacial CO₂ difference (e.g., Chalk *et al.*, 2017; Hönisch *et al.*, 2009). Chalk *et al.* (2017) concludes that the MPT was initiated by a change in ice sheet dynamics and that longer and higher-ice volume post-MPT ice ages are sustained by carbon cycle feedbacks, in particular dust fertilization of the Southern Ocean. That fact that our LR04-based prediction of CO₂ captures this same trend, of declining glacial CO₂, reflects that LR04 benthic stack also features an increase in the interglacial to glacial benthic $\delta^{18}\text{O}$ difference across the MPT, which is dominated by the glacial decline (Fig 3A.). Here, a comparison of PRED-CO₂ to a realised continuous oldest ice core record will be of value. The agreement or disagreement would inform on the proportionality of the CO₂ coupling with ice volume; if there were a major new or non-

478

479 linear process across the MPT that changed the nature of coupling between CO₂ and ice volume the PRED-CO₂ and
480 observed CO₂ records would be expected to diverge.
481
482 Another avenue to use the PRED-CO₂ record for hypothesis testing on the cause of the MPT concerns the phase locking
483 hypothesis. The phase locking hypothesis is proposed to explain the absence of precession-related (23 kyr) periods in the
484 LR04 benthic stack prior to the MPT (Fig 1), despite the strong precession cycle in insolation (Raymo *et al.*, 2006, Morée *et*
485 *al.*, 2021). The key concept is that prior to the MPT the Northern Hemisphere and Antarctic ice sheets were responsive (in
486 ice volume) to insolation changes in the precession band, but because precession forcing is out of phase between the
487 hemispheres, the ice volume changes were opposing between the hemispheres and therefore cancelled in the benthic stack.
488 This cancellation of the precession signal left insolation forcing in the 41 kyr obliquity band to dominate globally integrated
489 ice volume changes expressed in the benthic stack. A transition from a smaller and more dynamic terrestrial-terminating
490 Antarctic ice sheet to a larger and more stable marine-terminating ice sheet with cooling climate across the MPT (e.g.
491 Elderfield *et al.*, 2012) is then proposed to remove sensitivity of Antarctic ice volume to precession forcing and to suppress
492 ice sheet sensitivity to the obliquity band in favour of quasi-100kyr ice volume changes that are in phase between the
493 hemispheres (Raymo *et al.*, 2006).
494
495 Recently presented data from Yan *et al.* (2022), lend some support to the phase locking hypothesis, specifically with
496 evidence that pre-MPT Antarctic temperature (and by extension ice volume) is positively correlated with a local precession-
497 band insolation proxy based on the oxygen to nitrogen ratio of trapped air (Yan *et al.*, 2022). Whereas the correlation
498 becomes negative in the blue ice and continuous ice core data in the post-MPT record. If Yan *et al.*, (2022) is correct and the
499 phase locking hypothesis holds, then an implication is that prior to the MPT, Antarctic climate, Antarctic ice volume and by
500 extension Southern Ocean climate conditions, would fall out of phase with the LR04 benthic stack. To now extend the
501 argument to potential impacts on CO₂ exchange, if the phase locking hypothesis holds, then prior to the MPT the Antarctic
502 and Southern Ocean climate conditions and by extension the Southern Ocean mechanisms of CO₂ exchange described
503 earlier, would also be expected to fall out of phase with the benthic stack. Since our regression model assumes continuation
504 of the in-phase relationship between the benthic stack and Antarctic and Southern Ocean climate conditions (as inherited
505 from the post-MPT training data) we would expect to see major disagreement between our pre-MPT CO₂ predictions and a
506 realised oldest ice continuous ice core CO₂ record.

508 **Conclusions**

509 Here we have presented a predicted CO₂ record extending past the MPT. Our predictions are based on the relationships between
510 CO₂, sea-level, global ice volume and ocean temperature over the past 800 ky and therefore assume that these relationships

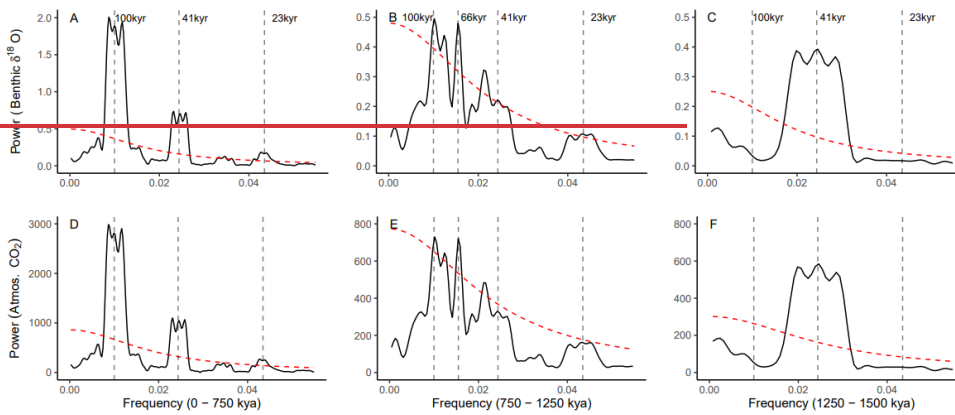
511 have remained constant from 800–1500 kya; this has defined our null hypothesis. The departure of our predicted CO₂ record
512 across the MPT from existing sparse data outside of the current continuous record reveals that climate–carbon cycle–
513 cryosphere relationships over the last 800 ky do not apply across and prior to the MPT. Our results provide quantitative
514 support of a fundamental change in the internal carbon–climate feedback systems of the earth over the Mid-
515 Pleistocene Transition. Comparison of the predictions from our simple model to real data, once gathered, from 1.5 my old
516 ice will provide further constraints on the processes involved in the MPT.

517 Summary and Conclusions

519 In this study we have used a simple generalised least squares (GLS) model to predict atmospheric CO₂ from the LR04
520 benthic δ¹⁸O stack for the period spanning the mid-Pleistocene transition, 800–1500 kyr. Our CO₂ prediction is therefore
521 based on the assumption that the physical processes linking CO₂, sea level, global ice volume and ocean temperature over the
522 past 800 kyr do not fundamentally change across the 800–1500 kya time period. The null-hypothesis is deliberately
523 simplistic on the basis that differences between our predictions and observed or proxy CO₂ records may be revealing of the
524 physical processes involved in the mid-Pleistocene Transition.

526 We made initial tests of the null hypothesis by comparing our predicted CO₂ record to existing discrete blue ice CO₂ records
527 and other non-ice-core proxy-CO₂ records from the 800–1500 kyr interval. Our predicted CO₂ concentrations do not show
528 any systematic departure from observed blue ice CO₂ concentrations. The predictions are marginally lower (during glacial
529 and interglacial stages) than those observed in blue ice from 1000 ± 89 kya and marginally higher than observed in blue ice
530 data from 1.5 Mya ± 213 kyr. Our predictions were generally lower than interglacial δ¹¹B-based-CO₂ reconstructions, but
531 higher than recent δ¹³C of leaf-wax based CO₂ reconstructions. Overall, we do not find clear evidence from the existing blue
532 ice or proxy CO₂ data to reject our predictions nor our associated null-hypothesis. The definitive test of our and other CO₂
533 predictions therefore awaits the future analysis of the upcoming continuous oldest ice core records. The PRED-CO₂ record
534 presented here should provide a useful comparison to forthcoming oldest ice core records and opportunity to provide further
535 constraints on the processes involved in the MPT.

537 **Appendices**



538

539 **Figure A:** Thomson-Multi-taper Method (MTM) spectral analysis representing relative power of signal periodicity for:
540 **A)** Benthic $\delta^{18}\text{O}$ after the Mid-Pleistocene Transition (MPT); **B)** Benthic $\delta^{18}\text{O}$ across the MPT (800–1250 kya); **C)**
541 **Benthic $\delta^{18}\text{O}$ prior to the onset of the MPT (1250 kya–1500 kya); **D)** CO_2 after the MPT; **E)** CO_2 across the MPT; **F)**
542 **CO_2 prior to the onset of the MPT. Each with a robust AR (1) 95% Confidence interval (red dashed line).****

543 **Author contributions**

544 **Project design by Jordan R.W. Martin, Joel Pedro, Tessa R. Vance. Data analysis and writing led by Jordan Martin with**
545 **contributions from Joel Pedro and Tessa R. Vance.**

546 **Project design by JRWM, JBP and TRV. Data analysis and writing led by JRWM with contributions from all**
547 **authors.**

548

549 **Competing interests**

550 The authors declare that they have no competing interests.

551 **Disclaimer**

552 This study, to the best of the author(s) knowledge and belief, contains no material previously published or written by another
553 person, except where due reference is made in the text of the study.

554 **Acknowledgements**

555 We acknowledge assistance from Simon Wotherspoon (Institute for Marine and Antarctic Studies) in appropriate model
556 selection methods. ~~We further acknowledge Chalk *et al.* and Higgins *et al.* for making the data from their respective studies
557 available for use in this study. Data will be publicly archived during the review process and by publication. This research was
558 supported by the Australian Government through Australian Antarctic Science projects 4632, the Million Year Ice Core
559 (MYIC) Project and by the Australian Government Department of Industry Science Energy and Resources, grant ASCI000002.~~

560

561 **Data availability**

562 ~~PRED-CO2 data will be publicly archived at the Australian Antarctic Data Centre (<https://data.aad.gov.au/> >>full link
563 provided upon publication<<).~~

564 ~~Data will be publicly archived during the review process and by publication.~~

565 **References**

566 Archer, D., Winguth, A., D. Lea, and Mahowald, N.: What caused the glacial/interglacial atmospheric pCO₂ cycle?, *Rev.*
567 *Geophys.*, 38, 159–189, 2000, <https://doi.org/10.1029/1999RG000066>, 2000.

568
569 Bazin, L., Landais, A., Lemieux-Dudon, B., Toyé Mahamadou Kele, H., Veres, D., Parrenin, F., Martinerie, P., Ritz, C.,
570 Capron, E., Lipenkov, V., Loutre, M.-F., Raynaud, D., Vinther, B., Svensson, A., Rasmussen, S., Severi, M., Blunier, T.,
571 Leuenberger, M., Fischer, H., Masson-Delmotte, V., Chappellaz, J., and Wolff, E.: An optimized multi-proxies, multi-site
572 Antarctic ice and gas orbital chronology (AICC2012): 120-800 ka, *Clim. Past*, 9, 1715-1731, [https://doi.org/10.5194/cp-9-](https://doi.org/10.5194/cp-9-1715-2013)
573 1715-2013, 2013.

574

575 Bereiter, B., Eggleston, S., Schmitt, J., Nehrbass-Ahles, C., Stocker, T. F., Fischer, H., Kipfstuhl, S., and Chappellaz, J.:
576 Revision of the EPICA Dome C CO₂ record from 800 to 600 ky before present, *Geophys. Res. Lett.*, 42, 542-549, doi:
577 10.1002/2014gl061957, 2015.

578
579 Berends, C. J., de Boer, B., and van de Wal, R. S. W.: Reconstructing the evolution of ice sheets, sea level, and atmospheric CO₂ during the
580 past 3.6 million years. *Clim. Past*, 17, 361–377, <http://doi.org/10.5194/cp-17-361-2021>, 2021a.

581

582 Berends, C. J., Köhler, P., Lourens, L. J., and van de Wal, R. S. W.: On the cause of the mid-Pleistocene transition., *Rev.*
583 *Geophys.*, 59, e2020RG000727, <https://doi.org/10.1029/2020RG000727>, 2021b.

584

585 Berger, A., Li, X. S., and Loutre, M. F.: Modelling northern hemisphere ice volume over the last 3Ma, *Quat. Sci. Rev.*, 18, 1-
586 11, doi: 10.1016/S0277-3791(98)00033-X, 1999.

Formatted: Normal, Line spacing: single

Formatted: Left

587
588 [Broecker, W.S.: Glacial to interglacial changes in ocean chemistry, *Prog. Oceanogr.*, 11 \(2\), 151-197.](#)
589 [https://doi.org/10.1016/0079-6611\(82\)90007-6](https://doi.org/10.1016/0079-6611(82)90007-6), 1982.
590
591 Chalk, T., Hain, M., Foster, G., Rohling, E., Sexton, P., Badger, M., Cherry, S., Hasenfratz, A., Haug, G., Jaccard, S., Martínez-
592 García, A., Pälike, H., Pancost, R., and Wilson, P.: Causes of ice age intensification across the Mid-Pleistocene Transition,
593 *Proc. Natl. Acad. Sci. U.S.A.*, 114, 13114-13119, doi: 10.1073/pnas.1702143114, 2017.
594
595 Clark, P. U., Archer, D., Pollard, D., Blum, J. D., Rial, J. A., Brovkin, V., Mix, A. C., Pisias, N. G., and Roy, M.: The middle
596 Pleistocene transition: characteristics, mechanisms, and implications for long-term changes in atmospheric pCO₂, *Quat. Sci.*
597 *Rev.*, 25, 3150-3184, doi: 10.1016/j.quascirev.2006.07.008, 2006.
598
599 Clark, P. U. and Pollard, D.: Origin of the Middle Pleistocene Transition by ice sheet erosion of regolith, *Paleoceanography*,
600 13, 1-9, doi: 10.1029/97pa02660, 1998.
601
602 [Dyez, K.A., Hönlisch, B., and Schmidt, G.A.: Early Pleistocene obliquity-scale pCO₂ variability at ~1.5 million years](#)
603 [ago. *Paleoceanogr. Paleoclimatol.*, 33, no. 11, 1270-1291, <https://doi.org/10.1029/2018PA003349>, 2018.](ago. Paleoceanogr. Paleoclimatol., 33, no. 11, 1270-1291, https://doi.org/10.1029/2018PA003349)
604
605 [Elderfield, H., Ferretti, P., Greaves, S., Crowhurst, S., McCave, N., and Piotrowski, A.M.: Evolution of Ocean Temperature](#)
606 [https://doi.org/10.1126/science.1221294](and Ice Volume Through the Mid-Pleistocene Climate Transition. <i>Science</i>, 337,704-709,
607 <a href=), 2012.
608
609 [Gottschalk, J., Battaglia, G., Fischer, H., Frölicher, T.L., Jaccard, S.L., Jeltsch-Thömmes, A., Joos, F., Köhler, P., Meissner,](#)
610 [K.J., Menviel, L., Nehrbass-Ahles, C., Schmitt, J., Schmittner, A., Skinner, L.C., and Stocker, T.G.: Mechanisms of](#)
611 [https://doi.org/10.1016/j.quascirev.2019.05.013](millennial-scale atmospheric CO₂ change in numerical model simulations, <i>Quaternary. Sci. Rev.</i>, 220, 30-74,
612 <a href=), 2019.
613
614 [Guillermic, M., Misra, S., Eagle, R., and Tripathi, A.: Atmospheric CO₂ estimates for the Miocene to Pleistocene based on](#)
615 [207, <https://doi.org/10.5194/cp-18-183-2022>, 2022.](foraminiferal δ¹¹B at Ocean Drilling Program Sites 806 and 807 in the Western Equatorial Pacific. <i>Clim. Past</i>, 18(2), 183-
616 <a href=)
617
618 Hasenfratz, A. P., Jaccard, S. L., Martínez-García, A., Sigman, D. M., Hodell, D. A., Vance, D., Bernasconi, S. M., Kleiven,
619 H. F., Haumann, F. A., and Haug, G. H.: The residence time of Southern Ocean surface waters and the 100,000-year ice age
620 cycle, *Science*, 363, 1080, doi: 10.1126/science.aat7067, 2019.
621
622 [Henehan, M. J., Rae, J. W. B., Foster, G. L., Erez, J., Prentice, K. C., Kucera, M., Bostock, H. C., Martínez-Botí, M. A.,](#)
623 [Milton, J. A., Wilson, P. A., Marshall, B. J., and Elliott, T.: Calibration of the boron isotope proxy in the planktonic](#)
624 [10.1016/j.epsl.2012.12.029](foraminifera <i>Globigerinoides ruber</i> for use in palaeo-CO₂ reconstruction, <i>Earth Planet. Sci. Lett.</i>, 364, 111-122, doi:
625 <a href=), 2013.
626
627 Higgins, J. A., Kurbatov, A. V., Spaulding, N. E., Brook, E., Introne, D. S., Chimiak, L. M., Yan, Y., Mayewski, P. A., and
628 Bender, M. L.: Atmospheric composition 1 million years ago from blue ice in the Allan Hills, Antarctica, *Proc. Natl. Acad.*
629 *Sci. U.S.A.*, 112, 6887, doi: 10.1073/pnas.1420232112, 2015.
630
631 Hönlisch, B., Hemming, N. G., Archer, D., Siddall, M., and McManus, J. F.: Atmospheric Carbon Dioxide Concentration
632 Across the Mid-Pleistocene Transition, *Science*, 324, 1551, doi: 10.1126/science.1171477, 2009.
633
634 International Panel on Climate Change: Climate change 2001; IPCC third assessment report, IPCC, Geneva, 2001.
635

Formatted: Left

Formatted: Font color: Text 1

636 International Partnerships in Ice Core Sciences: The oldest ice core: A 1.5 million year record of climate and greenhouse gases
637 from Antarctica [White paper]. IPICS, 2020.
638
639 Jouzel, J., Masson-Delmotte, V., Cattani, O., Dreyfus, G., Falourd, S., Hoffmann, G., Minster, B., Nouet, J., Barnola, J. M.,
640 Chappellaz, J., Fischer, H., Gallet, J. C., Johnsen, S., Leuenberger, M., Loulergue, L., Luethi, D., Oerter, H., Parrenin, F.,
641 Raisbeck, G., Raynaud, D., Schilt, A., Schwander, J., Selmo, E., Souchez, R., Spahni, R., Stauffer, B., Steffensen, J. P., Stenni,
642 B., Stocker, T. F., Tison, J. L., Werner, M., and Wolff, E. W.: Orbital and Millennial Antarctic Climate Variability over the
643 Past 800,000 Years, *Science*, 317, 793, doi: 10.1126/science.1141038, 2007.
644
645 Lisiecki, L. E. and Raymo, M. E.: A Pliocene-Pleistocene stack of 57 globally distributed benthic $\delta^{18}\text{O}$ records,
646 *Paleoceanography*, 20, PA1003, doi: 10.1029/2004pa001071, 2005.
647
648 [Martínez-García, A., Sigman, D.M., Ren, H., Anderson, R.F., Straub, M., Hodell, D.A., Jaccard, S.L., Eglinton, T.I., and](#)
649 [Haug, G.H.: Iron fertilization of the subantarctic ocean during the last ice age. *Science*, 343 \(6177\), 1347-1350,](#)
650 <https://doi.org/10.1126/science.1246848>, 2014.
651
652 [McClymont, E.L., Sosdian, S.M., and Rosell-Melé, A.: Pleistocene sea-surface temperature evolution: Early cooling,](#)
653 [delayed glacial intensification, and implications for the mid-Pleistocene transition. *Earth. Sci. Rev.*, 123, 173-193,](#)
654 <https://doi.org/10.1016/j.earscirev.2013.04.006>, 2013.
655
656 [Millero, F. J.: Thermodynamics of the carbon dioxide system in the oceans, *Geochim. Cosmochim. Acta.*, 59, 661-677,](#)
657 [https://doi.org/10.1016/0016-7037\(94\)00354-O](https://doi.org/10.1016/0016-7037(94)00354-O), 1995.
658
659 [Morée, A. L., Sun, T., Bretones, A., Straume, E. O., Nisancioglu, K., and Gebbie, G.: Cancellation of the precessional cycle](#)
660 [in \$\delta^{18}\text{O}\$ records during the Early Pleistocene. *Geophys. Res. Lett.*, 48,](#)
661 [e2020GL090035. https://doi.org/10.1029/2020GL090035](https://doi.org/10.1029/2020GL090035), 2021.
662
663 Petit, J. R., Jouzel, J., Raynaud, D., Barkov, N. I., Barnola, J. M., Basile, I., Bender, M., Chappellaz, J., Davis, M., Delaygue,
664 G., Delmotte, M., Kotlyakov, V. M., Legrand, M., Lipenkov, V. Y., Lorius, C., Pépin, L., Ritz, C., Saltzman, E., and
665 Stievenard, M.: Climate and atmospheric history of the past 420,000 years from the Vostok ice core, Antarctica, *Nature*, 399,
666 429-436, doi: 10.1038/20859, 1999.
667
668 Raymo, M., Lisiecki, L., and Nisancioglu, K.: Plio-Pleistocene Ice Volume, Antarctic Climate, and the Global 18O Record,
669 *Science*, 313, 492-495, doi: 10.1126/science.1123296, 2006.
670
671 Raymo, M., Ruddiman, W., and Froelich, P.: Influence of Late Cenozoic mountain building on ocean geochemical cycles,
672 *Geology*, 16, 649-653, doi: 10.1130/0091-7613(1988)016<0649:IOLCMB>2.3.CO;2, 1988.
673
674 Raymo, M. E.: The timing of major climate terminations, *Paleoceanography*, 12, 577-585, doi: 10.1029/97PA01169, 1997.
675
676 Raymo, M. E. and Huybers, P.: Unlocking the mysteries of the ice ages, *Nature*, 451, 284-285, doi: 10.1038/nature06589,
677 2008.
678
679 [Rohling, E. J., Foster, G. L., Grant, K. M., Marino, G., Roberts, A. P., Tamisiea, M. E., and Williams, F.: Sea level and deep-](#)
680 [sea temperature variability over the past 5.3 million years, *Nature*, 508, 477-482, doi: 10.1038/nature13230](#), 2014.
681
682 Ruddiman, W. F., Raymo, M. E., Martinson, D. G., Clement, B. M., and Backman, J.: Pleistocene evolution: Northern
683 hemisphere ice sheets and North Atlantic Ocean, *Paleoceanography*, 4, 353-412, doi: 10.1029/PA004i004p00353, 1989.
684

Formatted: Left

Formatted: Font: Font color: Text 1, English (United Kingdom)

685 [Röthlisberger, R., Bigler, M., Wolff, E. W., Joos, F., Monnin, E., and Hutterli, M. A.: Ice core evidence for the extent of past](#)
686 [atmospheric CO₂ change due to iron fertilisation, *Geophys. Res. Lett.*, 31, L16207,](#)
687 <https://doi.org/10.1029/2004GL020338>, 2004.

688

689 [Ruddiman, W. F., Raymo, M. E., Martinson, D. G., Clement, B. M., and Backman, J.: Pleistocene evolution: Northern](#)
690 [hemisphere ice sheets and North Atlantic Ocean, *Paleoceanography*, 4, 353–412, https://doi.org/10.1029/PA004i004p00353,](#)
691 [1989.](#)

692

693 [Shackleton, N. J. and Pisias, N. G.: Atmospheric Carbon Dioxide, Orbital Forcing, and Climate. In: *The Carbon Cycle and*](#)
694 [Atmospheric CO₂: Natural Variations Archean to Present](#), https://doi.org/10.1029/GM032p0303, 1985.

695

696 [Shugi, H., The older the ice, the better the science. *Adv. Polar Sci.*, 23, 121–122, https://doi.org/10.13679/j.advps.2022.0004,](#)
697 [2022.](#)

698

699 [Stephens, B.B., Keeling, R.F.: The influence of Antarctic sea ice on glacial–interglacial CO₂ variations. *Nature*, 404, 171–](#)
700 [174, https://doi.org/10.1038/35004556](#), 2000.

701

702 [Tzedakis, P. C., Crucifix, M., Mitsui, T., and Wolff, E. W.: A simple rule to determine which insolation cycles lead to](#)
703 [interglacials, *Nature*, 542, 427–432, doi: 10.1038/nature21364](#), 2017.

704

705 [Ushie, H., and Matsumoto, K.: The role of shelf nutrients on glacial-interglacial CO₂: A negative feedback, *Global*](#)
706 [Biogeochem. Cy., 26, GB2039, https://doi.org/10.1029/2011GB004147., 2012.](#)

707

708 [van de Wal, R. S. W., de Boer, B., Lourens, L. J., Köhler, P., and Bintanja, R.: Reconstruction of a continuous high-](#)
709 [resolution CO₂ record over the past 20 million years. *Clim. Past*, 7, 1459–1469, https://doi.org/10.5194/cp-7-1459-2011,](#)
710 [2011.](#)

711

712 [Veres, D., Bazin, L., Landais, A., Toyé Mahamadou Kele, H., Lemieux-Dudon, B., Parrenin, F., Martinerie, P., Blayo, E.,](#)
713 [Blunier, T., Capron, E., Chappellaz, J., Rasmussen, S., Severi, M., Svensson, A., Vinther, B., and Wolff, E.: The Antarctic](#)
714 [ice core chronology \(AICC2012\): an optimized multi-parameter and multi-site dating approach for the last 120 thousand](#)
715 [years, *Clim. Past*, 9, 1733–1748, https://doi.org/10.5194/cp-9-1733-2013](#), 2013.

716

717 [Willeit, M., Ganopolski, A., Calov, R., and Brovkin, V.: Mid-Pleistocene transition in glacial cycles explained by declining](#)
718 [CO₂ and regolith removal, *Sci. Adv.*, 5, eaav7337, doi: 10.1126/sciadv.aav7337](#), 2019.

719

720 [Wolff, E. W., Chappella, J., Fischer, H., Kull, C., Miller, H., Stocker, T. F., and Watson, A. J.: The EPICA challenge to the](#)
721 [Earth system modeling community, *Eos \(Washington DC\)*, 85, 363363, doi: 10.1029/2004EO380003](#), 2004.

722

723 [Wolff, E. W., Kull, C., Chappellaz, J., Fischer, H., Miller, H., Stocker, T. F., Watson, A. J., Flower, B., Joos, F., Köhler, P.,](#)
724 [Matsumoto, K., Monnin, E., Mudelsee, M., Paillard, D., and Shackleton, N.: Modeling past atmospheric CO₂: results of a](#)
725 [challenge, *EOS*, 86 \(38\), 341–345, http://doi.org/10.1029/2005EO380003](#), 2005.

726

727 [Yamamoto, M., Clemens, S.C., Seki, O., Tsuchiya, Y., Huang, Y., O’ishi, R., and Abe-Ouchi, A.: Increased interglacial](#)
728 [atmospheric CO₂ levels followed the mid-Pleistocene Transition, *Nat. Geosci.*, 15\(4\), 307–313,](#)
729 <https://doi.org/10.1038/s41561-022-00918-1>, 2022.

730

731 [Yan, Y., Bender, M.L., Brook, E.J., Clifford, H.M., Kameny, P.C., Kurbatov, A.V., Mackay, S., Mayewski, P.A., Ng, J.,](#)
732 [Severinghaus, J.P., and Higgins, J.A.: Two-million-year-old snapshots of atmospheric gases from Antarctic ice, *Nature*,](#)
733 [574\(7780\), 663–666, https://doi.org/10.1038/s41586-019-1692-3](#), 2019.

734

Formatted: Left

Formatted: Font: Font color: Text 1, English (United Kingdom)

Formatted: Left

735 Yan, Y., Kurbatov, A.V., Mayewski, P.A., Shackleton, S., and Higgins, J.A.: Early Pleistocene East Antarctic temperature in
736 phase with local insolation. Nat. Geosci., 16, 50-55, <https://doi.org/10.1038/s41561-022-01095-x>, 2022.
737
738